Characteristic X-Ray Production in Magnesium, Aluminum, and Copper by Low-Energy Hydrogen and Helium Ions*

Werner Brandt, Roman Laubert, and Ivan Sellin

Department of Physics, New York University, New York, New York

(Received 15 June 1966)

Comparative characteristic K x-ray yields in Mg and Al and, L x-ray yields in Cu, produced by bombardment with singly charged ions of H, He^3, and He^4, are reported for particle energies ranging from 25 to 50 keV per amu. Characteristic x-ray production cross sections for the K-shell processes are extracted from these data, and from previous proton work. The ratios of helium to proton cross sections at equal particle velocities are significantly smaller than expected from current theories. It is shown that the discrepancy can be fully accounted for by the effect on the cross section of the binding of the K-shell electrons to the projectile, which is in close proximity to the nucleus at the time of excitation.

INTRODUCTION

PREVIOUS measurements of the characteristic x-ray yields from the K shells of Mg, Al, and Cu, as observed by Khan, Potter, and Worley[1] with protons in the range from 15 to 1900 keV, lead to production cross-sections which fall short of the theoretical cross-sections calculated in Born approximation.[2,3] The discrepancy is attributed to the deflection of the impinging projectile in the Coulomb field of the target nucleus as derived by Bang and Hansteen.[4] The Coulomb-deflection is of much greater importance in the present context than is usual for atomic collision processes generally, because the matrix elements for inner-shell ionization processes are large only at distances of approach small compared with the relevant shell radii. In the course of a systematic study of these Coulomb-deflection effects on characteristic x-ray yields, by using projectiles of different masses at equal velocities, we uncovered an additional effect which can reduce the cross sections substantially. Under certain conditions this effect can outweigh the effects of the Coulomb-deflection.

We report the experimental details in Sec. 1. The data are analyzed and discussed in Sec. 2. Section 3 presents our interpretation and conclusions.

1. APPARATUS AND EXPERIMENTAL METHOD

The experimental arrangement employed is shown in Fig. 1. The ions are created and accelerated in our heavy-ion accelerator[5] to energies ranging from 25 to 200 keV. The particles are then mass and energy analyzed in a 10-kG magnetic spectrometer similar to the one described by White and his co-workers.[6] The energy spread of the ions striking the targets is less than 1% at all energies.

The targets consist of 2–5 mil high-purity (>99.99%) metal foils. The target is mounted on a holder with its surface inclined at 45° to the ion beam, and to the direction of the proportional counter window. The target holder, insulated thermally and electrically from the target chamber, can be heated and cooled. The temperature of the target, monitored via a thermocouple in good contact with the foil, can be regulated to ±3°C. The target chamber, pumped by a 280-liter/sec turbo-molecular pump located 18 in. from the target, is kept at a pressure of less than 5×10^{-6} Torr under all operating conditions. A positive bias relative to ground prevents the escape of secondary electrons ejected by the impinging ions. An electrometer coupled with a current integrator records the total charge deposited by the ion beam to an accuracy of ±2%. The emitted x-ray quanta are counted by a flow-mode proportional counter similar to the one described by Khan and Potter.[7] After amplification, a multichannel an-
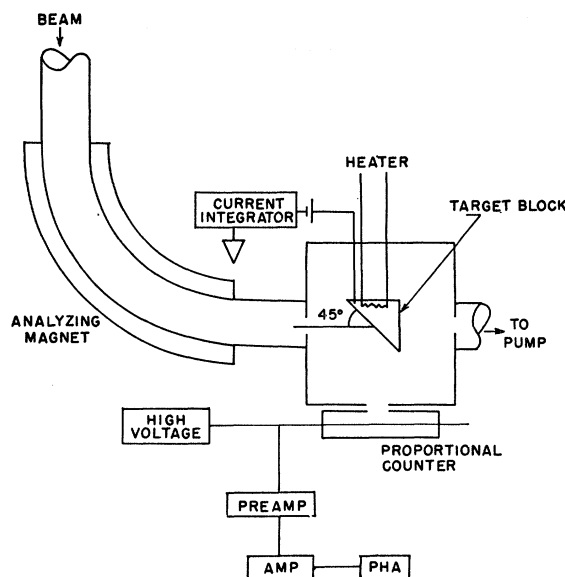
FIG. 1. Schematic diagram of the apparatus.

[1] J. M. Khan, D. L. Potter, and R. D. Worley, Phys. Rev. 139, A1735 (1965).

[2] T. Huus, J. Bjerregaard, and B. Elbek, Kgl. Danske Videnskab. Selskab, Mat. Fys. Medd. 30, 17 (1956).

[3] For a general review, cf. E. Merzbacher and H. W. Lewis, *Encyclopedia of Physics*, edited by S. Flügge (Springer-Verlag, Berlin, 1958), Vol. 34, p. 166.

[4] J. Bang and J. M. Hansteen, Kgl. Danske Videnskab. Selskab, Mat. Fys. Medd. 31, No. 13 (1959).

[5] R. Laubert and N. Wotherspoon, IEEE Trans. Nucl. Sci. 12, 285 (1965).

[6] F. A. White, F. M. Rourke, and J. C. Sheffield, Appl. Spectry. 12, 46 (1958).

[7] J. M. Khan and D. L. Potter, Phys. Rev. 133, A890 (1964).

alyzer stores the counter pulses. We use a standard counting gas consisting of a 90% argon and 10% methane mixture. The counter window of approximately 1 cm diam is covered with a 0.35-mil aluminized Mylar window. The counter calibration is performed and checked during all experimental runs with the 6.4-keV x rays from a Co[57] source.

The beam spot size at the target is kept at approximately 0.15 cm diam, with a beam current of $\sim 3 \times 10^{-8}$ A. At this current our geometry permits, for example, an Al(K) spectrum for 175-keV protons of 10^5 counts to be collected in one minute. By contrast, in exciting with He[4] at 100 keV, several hours of exposure are required to separate a clearly defined x-ray spectrum from the background.

The relative x ray yields for singly charged He[4] ions and protons are measured consecutively at a preset machine energy by using a helium-hydrogen gas mixture in the ion source of the accelerator. For the He[3] measurements, a mixture of He[3] and He[4] gas is fed into the ion source. In this method of concurrent comparison the errors associated with current and energy measurements are minimized.

The metal foils are cleaned in alcohol and distilled water before installation in the target holder. After outgassing *in vacuo* at 250°C, the foils are maintained at 150°C to suppress carbon deposition during irradiation. Khan et al.[1] have studied the problem of carbon deposition extensively with protons and found the carbon layer build-up to be proportional to the proton dose imparted to the target. We have studied the carbon deposition by monitoring the Al(K) x-ray yield for given beam current and energy, as a function of the total beam charge collected at the target, for different target temperatures. Two such runs are shown in Fig. 2, measured without the turbo-molecular pump on the target chamber, for target temperatures 8°C and 100°C. Similar results are obtained with the pump, but the 8°C slope, e.g., is then reduced to $\frac{1}{10}$ of that in Fig. 2. In any case we find for our beam characteristics that at target temperatures above 100°C the carbon build-up becomes negligible, while the characteristic x-ray yield of the target proper remains independent of temperature. We have confirmed this explicitly over the temperature range 0°–400°C. It is the energy loss of the impinging particles in the carbon layer which causes the diminution of the target x-ray yield at temperatures lower than approximately 100°C.

2. RESULTS

Our yield data for various particle-target combinations are shown in Figs. 3 and 4. In each graph the accumulated counts from the pulse-height analyzer, at a preset integrated beam current, are plotted against the beam energy, after corrections for background and dead time. We extract relative cross sections in a standard manner according to the formula[3]

$$\sigma(E_1) = N_2^{-1}[(dY(E)/dE)_{E_1}S_2(E_1) + \mu_2 Y(E_1)], \quad (1)$$
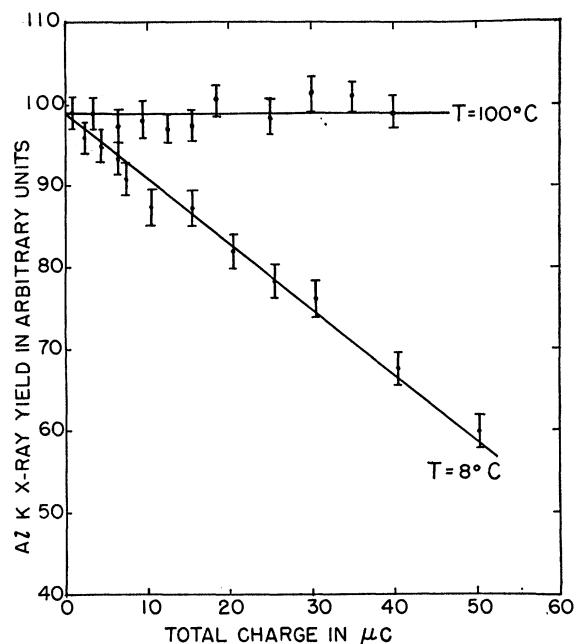
Fig. 2. Yield of Al(K) x rays in arbitrary units for 200-keV protons versus total integrated charge at 8°C and 100°C. The beam current density in both cases was 0.2 μA/cm².

where E_1 is the energy of the incoming particles, N_2 the target density, Y the yield, S_2 the stopping power, and μ_2 the absorption coefficient of the target for its own characteristic x rays. Our yield curves allow differentiation with regard to energy, with an uncertainty of $\lesssim 15\%$. It is the lack of accurate stopping-
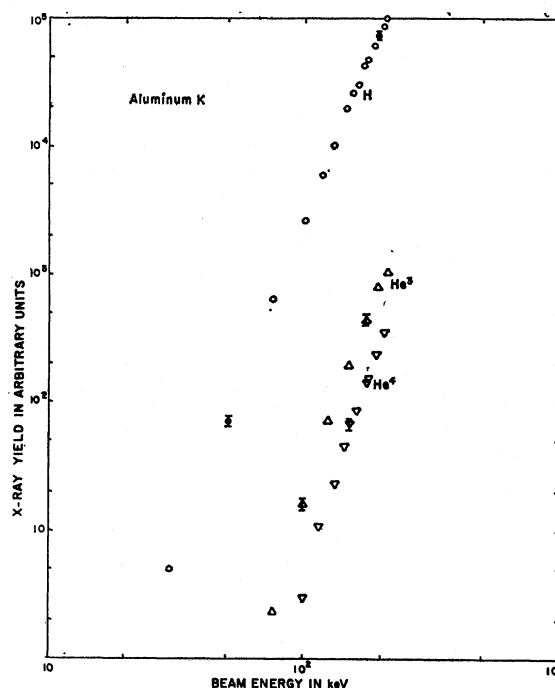
Fig. 3. Yield of Al(K) x rays in arbitrary units versus beam energy for H, He[3], and He[4] projectiles. Both scales are logarithmic.
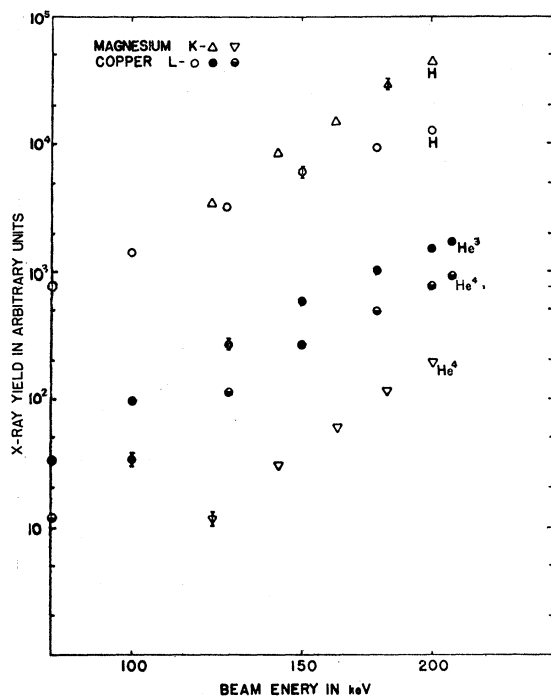
FIG. 4. Yield of Mg(K) x rays in arbitrary units versus beam energy for H and He^4 projectiles; yield of Cu(L) x rays in arbitrary units versus beam energy for H, He^3, and He^4 projectiles.

power data which is the limiting factor in our balance of errors. In the calculation we use two recent sets of stopping-power measurements for low-energy H and He ions in Al.[8,9] When we compare ratios of cross sections for different particles in the same target material, only the ratios of these stopping powers enter, which reduces the uncertainties considerably. We deduce a value ~ 2.6 for the ratio of the stopping powers of aluminum against He and H projectiles, both from the experiments cited and from the statistical model calculations of Lindhard and Scharff.[10] For $(Z_1/Z_2) \ll 1$, a criterion fulfilled in all our work, this stopping power ratio depends only weakly on Z_2, and is also used for magnesium. Cross sections in absolute units are then calculated by normalizing our relative data to those of Khan et al.[1] in choosing the proton cross section in aluminum at 100 keV, $(\sigma_H)_{Al(K)} = 1.54$ b as the standard value of reference. Should this standard need revision in the future, all our cross sections can be readjusted by mere multiplication with a constant factor. However, most of the discussion below centers on cross-section ratios which do not depend on the choice of any absolute standard.

The resulting characteristic x-ray production cross sections for various projectile-target combinations are listed in Table I. Ratios of some of these cross sections

[8] J. H. Ormrod, J. R. Macdonald, and H. E. Duckworth, Can. J. Phys. 43, 280 (1965).
[9] R. D. Moorhead, J. Appl. Phys. 36, 394 (1965).
[10] J. Lindhard and M. Scharff, Phys. Rev. 124, 128 (1961).

TABLE I. Cross sections for K-shell x-ray production for H, He^3, and He^4 projectiles in Mg and Al targets.

Beam energy in keV	Cross sections in barns[a] Mg target		Al target		
	σ_H	σ_{He^4}	σ_H	σ_{He^3}	σ_{He^4}
30			1.3(−2)		
50	2.3(−1)[b]		1.2(−1)		
80			7.4(−1)		
100			1.5(0)	3.8(−2)	6.1(−3)
125	8.3(0)	7.4(−2)	4.8(0)	1.3(−1)	3.1(−2)
150	1.5(1)	1.8(−1)	7.8(0)	2.6(−1)	8.6(−2)
175	2.6(1)	3.4(−1)	1.6(1)	4.4(−1)	1.7(−1)
200	4.0(1)	5.9(−1)	2.9(1)	6.8(−1)	3.1(−1)

[a] The cross sections are normalized to $(\sigma_H)_{Al(K)}$ of Ref. 1 at 100 keV. The appropriate power of 10 is contained in parentheses.
[b] This cross section was taken from Ref. 1 to allow comparison with our He^4 cross section at 200 keV.

at equal particle velocities are contained in Table II, with other entries to be discussed presently.

3. DISCUSSION

The cross section for K-shell ionization by slow heavy particles was derived by Huus, Bjerregaard, and Elbek[2] in Born approximation for particle orbits undeflected in the Coulomb field of the target nuclei. We write the result in atomic units as

$$\sigma_K{}^0 = C_{2K}(Z_1{}^2 Z_2{}^2/v_1)q_0{}^{-9}, \qquad (2)$$

where Z_1 is the atomic number of the incoming particle of velocity v_1 and energy E_1, Z_2 is the atomic number of the target atoms, and C_{2K} is a target constant. The electrons to be ejected initially are bound with an energy ω_{2K} in the target K shells of radius a_{2K}. The parameter $q_0 = \omega_{2K}/v_1$ is a measure of the slowness of the encounter in the sense that Eq. (2) applies for $a_{2K}q_0 \gg 1$. In comparing Eq. (2) with our experimental cross sections we take the fluorescence yield to be independent of the nature of the projectile. This should be a very good approximation for our targets where the fluorescence lifetimes τ are so long that $\tau\omega_{2K} \gg a_{2K}q_0$. Bang and Hansteen[4] derived the reduction of the differential ionization cross sections due to the Coulomb deflection. We incorporate their result to leading terms and

TABLE II. Comparison of cross sections for Mg and Al K-shell x-ray production for H, He^3, and He^4 ions at equal particle velocities.

Target	Al	Al	Mg
Beam energy in keV/amu	32	50	50
$(\sigma_{He^4}/\sigma_{He^3})_K$ with Coulomb effect	1.20	1.10	
experimental	1.2±0.1	1.2±0.1	
$(\sigma_{He^0}/4\sigma_H{}^0)_K$	1.00	1.00	1.00
$(\sigma_{He^4}/4\sigma_H)_K$ with Coulomb effect	1.63	1.29	1.26
with binding effect	0.35	0.36	0.33
with combined effects	0.57	0.46	0.42
experimental	0.6±0.1	0.6±0.1	0.6±0.1

find that

$$\sigma_K = 9E_{10}(\pi d q_0)\sigma_K^0, \qquad (3)$$

where $2d = Z_1 Z_2 / E_1$ is the minimum distance of closest approach; the exponential integral $E_{10}(x)$ is a tabulated function.[11]

On examining the He^3 and He^4 yield data displayed in Figs. 3 and 4, we find that the yields are approximately the same at equal particle velocities, the remaining discrepancy being just of the kind and magnitude expected from Eq. (3). For example, Table II shows that at 50 keV/amu, $(\sigma_{He^4}/\sigma_{He^3})_{Al(K)}$ $= 1.2 \pm 0.1$, to be compared with the value 1.10 derived from Eq. (3). These ratios are insensitive to the particle velocity, as in fact are all cross-section ratios extracted from our data. The experimental ratio $[\sigma_{He^4}/4\sigma_H]_{Al(K)}$ has a value close to 0.6. It plainly is at variance with the value 1.5 expected from Eq. (3).

We interpret these results as follows. The cross section σ_K^0 is so sensitive a function of the binding energy of the electrons to be ejected by the passing particle that the additional binding to the positive charge of the projectile affects the cross section markedly. We expect such an effect to show up in ratios such as (σ_{He^4}/σ_H) or (σ_{He^3}/σ_H) but not in ratios for different impinging isotopes, such as in $(\sigma_{He^4}/\sigma_{He^3})$, where the particle charges are equal. We estimate the increase in ω_{2K} due to the proximity of a particle charge $Z_1 \ll Z_2$ moving slowly at a distance r from the nucleus in first-order perturbation theory. Using hydrogenic wave functions with screening constants S, we find for the increment $\Delta\omega_K$ of the K-shell binding

$$\Delta\omega_K(r/a_{2K}) = \frac{2Z_1\omega_{2K}}{Z_2 - S_{2K}} \frac{a_{2K}}{r}$$

$$\times \left\{ 1 - \left(1 + \frac{r}{a_{2K}}\right)\exp\left(-\frac{2r}{a_{2K}}\right) \right\}. \quad (4)$$

We add Eq. (4) to ω_{2K} in the differential ionization cross-section for given impact parameter, and average over all impact parameters, using the probability distribution given by Bang and Hansteen for K-shell ionization as a function of impact parameter. Finally, we integrate over all final states of the ejected electrons. On omitting small terms we find

$$\sigma_K = 9\epsilon^{-9}E_{10}(\pi d q_0 \epsilon)\sigma_K^0, \qquad (5)$$

where $\epsilon = [1 + \Delta\omega_K(\sqrt{3}/q_0 a_{2K})/\omega_{2K}]$.

Since we consider conditions such that $q_0 a_{2K} \gg 1$, the function ϵ depends only weakly on the particle velocity. Referring to Eq. (4), under extreme low-energy conditions the inclusion of the effect of binding in Eq. (5) amounts to replacing $\omega_{2K}(Z_2)$ by $\omega_K(Z_1 + Z_2)$ $\cong \omega_{2K}(Z_2)[1 + Z_1/(Z_2 - S_{2K})]^2$ in the expression for q_0

[11] *Handbook of Mathematical Functions*, edited by M. Abramowitz and I. A. Stegun (U. S. Department of Commerce, National Bureau of Standards, Washington, D. C., 1964), Appl. Math. Ser. 55, Chap. 5, pp. 245 ff.
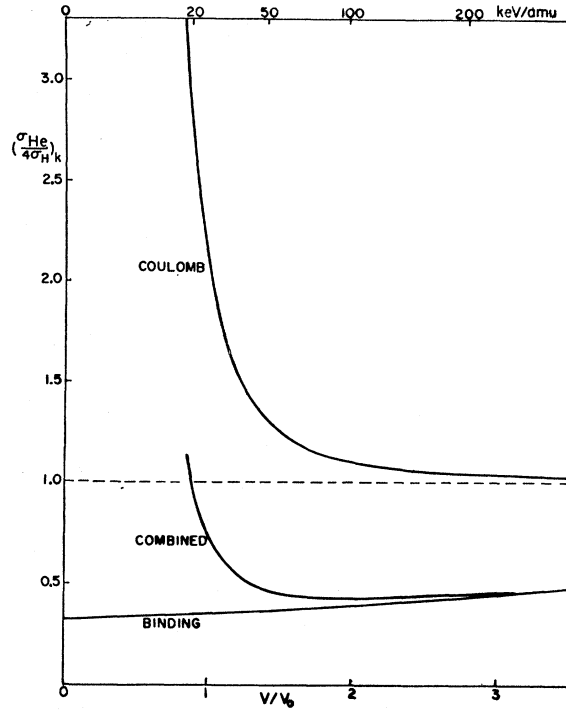
FIG. 5. The cross section ratio $(\sigma_{He^4}/4\sigma_H)_K$ calculated for Al in the four approximations discussed in the text.

in Eq. (3). Preliminary sample calculations suggest that under the same conditions this effect on L-shell ionizations can be accounted for in an approximate manner by similarly replacing in the cross sections $\omega_{2L}(Z_2)$ with $\omega_L(Z_1 + Z_2)$. The effect vanishes as $(Z_1/Z_2) \to 0$.

We have plotted in Fig. 5 the cross-section ratio $(\sigma_{He^4}/4\sigma_H)_{Al(K)}$ as a function of the particle velocity in the different approximations discussed here. The straight reference line derives from Eq. (2) and the "Coulomb" curve from Eq. (3). The straight-orbit approximation, $\sigma_K = \epsilon^{-9}\sigma_K^0$, in the "binding" curve, is modified by Eq. (5), via the Coulomb deflection to give the "combined" curve. The corresponding curves for the Mg K-shell would be indiscernibly close to those shown in Fig. 5 for Al. The "combined" cross-section ratios in the pertinent range of particle velocities agree with the corresponding experimental results as summarized in Table II. We find that the combined effects contained in Eq. (5) close the large gap between theory and experiment as noted, for example, by Khan and his co-workers[1] for protons on carbon and aluminum targets.

ACKNOWLEDGMENTS